ACS SYMPOSIUM SERIES 499

Supramolecular Architecture

Synthetic Control in Thin Films and Solids

Thomas Bein, EDITOR
Purdue University

Developed from a symposium sponsored
by the Division of Inorganic Chemistry
at the 201st National Meeting
of the American Chemical Society,
Atlanta, Georgia,
April 14–19, 1991

American Chemical Society, Washington, DC 1992

Chapter 2

Designing Ordered Molecular Arrays in Two and Three Dimensions

John P. Folkers, Jonathan A. Zerkowski, Paul E. Laibinis, Christopher T. Seto, and George M. Whitesides[1]

Department of Chemistry, Harvard University, Cambridge, MA 02138

Two- and three-dimensional assemblies — self-assembled monolayers (SAMs) and hydrogen-bonded co-crystals, respectively — show substantial changes in their supramolecular structures with seemingly minor changes in the structures of their molecular/atomic constituents. The structure of SAMs obtained by adsorption of alkanethiols onto silver and copper are indistinguishable, although the atomic radii of silver and copper are different. The structure of the SAM on silver is different from that on gold, although the atomic radii of these metals are essentially the same. A macroscopic property of the SAMs, wetting, is not affected by these structural differences. Co-crystals formed from derivatives of barbiturates and melamines form hydrogen-bonded tapes in the solid state. These tapes provide a template for studying the packing forces within crystals. The three-dimensional arrangement of the tapes in the crystals changes markedly in response to subtle differences in the steric and electronic structures of the molecular constituents.

The construction of large ensembles of molecules is a current challenge for molecular science. Although the design and synthesis of macromolecular ensembles in solution is well advanced *(1)*, development of corresponding techniques for the organic solid-state are more difficult and less well developed. We have started a program in designing solid-state structures based on inorganic and organic coordination chemistry.

Solution-phase patterns of reactivity in inorganic and organic chemistry are a starting point for the design of solid-state materials. We use both coordination and hydrogen bonds to design solids. In this paper we survey two approaches to the formation of solid-state structures: the application of inorganic coordination chemistry to the formation of self-assembled monolayers, and the design of three-dimensional crystals with controlled structures using networks of hydrogen bonds.

Self-Assembled Monolayers

Background. Self-assembled monolayers (SAMs) form by the spontaneous adsorption of ligands from solution onto the surface of a metal or metal oxide (*2,3*).

[1]Corresponding author

0097–6156/92/0499–0010$06.00/0

The processes involved in these adsorptions are related to coordination chemistry in solution, but occur in two dimensions. Metal surfaces can be viewed as planes of metal atoms having vacant coordination sites. Appropriate ligands coordinate (or, in the terms of surface science, adsorb) to a metal surface and form an ensemble that we and others refer to as a self-assembled monolayer. Adsorbates containing polymethylene chains are the most commonly studied because they often form oriented, highly ordered SAMs. Some of the presently available systems that yield SAMs include alkanoic acids on oxidized metal surfaces (especially aluminum) (*4*), alkyl amines on oxidized surfaces of chromium and platinum (*5*), isonitriles on platinum (*6*), sulfides (*7*), disulfides (*8–10*), and thiols (*11,12*), on gold, and thiols on silver (*13–15*). All of these systems have analogs in classical coordination chemistry (*16*).

SAMs on Gold. SAMs formed by the adsorption of alkanethiols onto gold surfaces are presently the best characterized of these systems. Our studies have employed evaporated gold films as substrates. The resulting surfaces of the gold are polycrystalline, and these crystallites are oriented in a way that presents predominantly the (111) crystal face (*9*). This face has the lowest surface free energy. Unlike most metals, gold does not form an oxide under ambient conditions. With gold as a substrate, the SAMs form on a polycrystalline metal rather than on an amorphous overlayer of oxide. These gold films do not require special handling or cleaning, and the resultant monolayers are stable to cleaning and manipulation.

The structure of SAMs derived from adsorption of n-alkanethiols ($HS(CH_2)_nCH_3$; n = 10-21) on gold has been determined using a variety of techniques (*11,12,15,17–22*). The adsorbed species is believed to be a gold(I) alkanethiolate ($RS^-Au(I)$) rather than an alkanethiol (RSH) (*15,22*); the mechanism of formation of the thiolate, however, has not been established. Transmission electron microscopy and diffraction (TEM) experiments determined the arrangement of thiolates on a gold (111) surface (*17*). On this surface, the sulfur atoms occupy three-fold hollow sites and form a hexagonal lattice. The lattice of sulfur atoms is displaced 30° relative to the gold (111) hexagon, and the intramolecular distances are $\sqrt{3}$ times larger than the interatomic distance of gold (*17,20*). This structure is referred to as $(\sqrt{3}x\sqrt{3})R30°$ (Figure 1a). The terminal methyl groups of the SAM also form a hexagonal lattice with the same intermolecular spacing as the sulfur atoms, as shown by low-energy helium diffraction (*18*) and scanning tunneling microscopy (*21*).

Polarized infrared external reflection spectroscopy (PIERS) has been very useful in determining the structural details of these SAMs (*11,15,20,21*). PIERS results show that SAMs of alkanethiolates on gold are nearly analogs of two-dimensional crystalline alkanes. The alkane chains are predominantly in a trans zig-zag conformation; the few gauche conformations are concentrated near the ends of the chains (*15,18,23*). The alkane chains are tilted ~26° relative to the surface normal. This tilt, which allows the chains to be close-packed, is a direct result of the lattice spacing of the sulfur atoms.

The high selectivity of the gold surface towards sulfur-containing groups allows a wide variety of functional groups to be incorporated into the assembly (*3,12,19,20,24,25*). In many cases, the highly-ordered structure of the SAM is preserved and two-dimensional ensembles of organic functional groups are formed. We have employed these functionalized monolayers in the study of wetting (*3,12,24,25*).

The wetting properties of the SAM are due almost entirely to the tail group (X) of the alkanethiol ($HS(CH_2)_nX$). For example, $X = CH_3$ yields a SAM that is oleophobic (advancing contact angle of hexadecane, $\theta_a(HD)$, ≈ 50°) and hydrophobic ($\theta_a(H_2O) \approx 115°$); $X = CO_2H$ or OH yields SAMs that are hydrophilic ($\theta_a(H_2O) < 15°$) (*12,24,25*). The wetting properties of these SAMs indicate that the tail group are

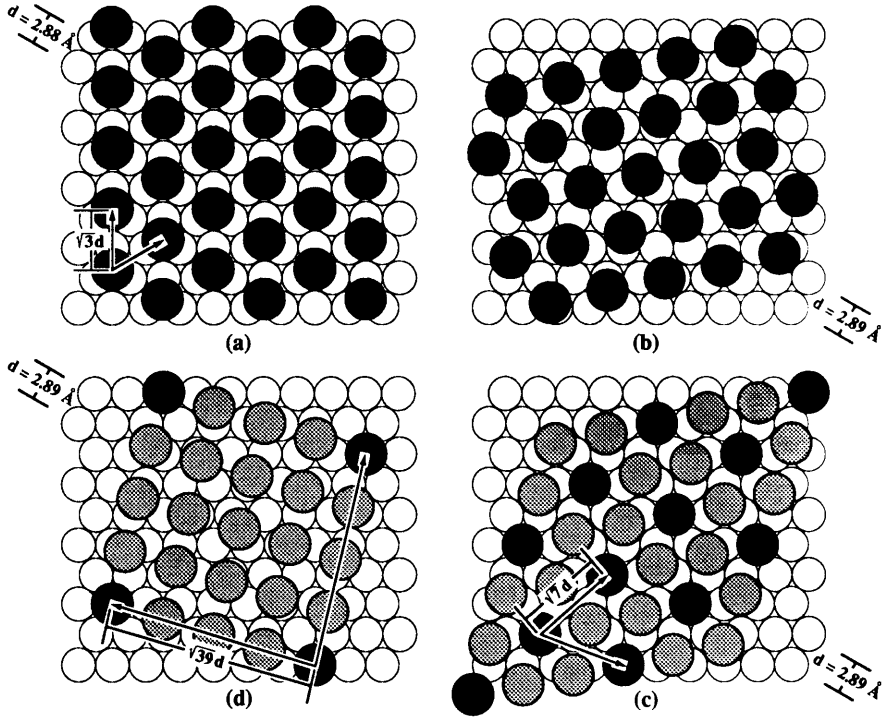

Figure 1. Schematic illustration of several of the lattices formed by the adsorption of sulfur-containing species onto gold and silver. In these figures, the small, open circles represent metal atoms in the (111) plane, black circles define the unit cell of sulfur atoms, and gray circles represent other sulfur atoms within the unit cell. (a) The $(\sqrt{3}x\sqrt{3})R30°$ lattice formed by the adsorption of long-chain alkanethiols onto gold (*17,20*); the surface species in this structure is RS⁻Au(I) (*15,22*). The area per sulfur atom is 21.5 $Å^2$. (b) Incommensurate lattice formed by the adsorption of octadecanethiol onto silver (*31*); the surface species is RS⁻Ag(I) (*14,15*). The area per sulfur atom in this structure is 19.1 $Å^2$. (c) The $(\sqrt{7}x\sqrt{7})R10.9°$ lattice formed by the adsorption of hydrogen sulfide onto silver (*32*) and by the adsorption of dimethyl disulfide onto silver (*33*); the surface species are S^{2-} and CH_3S⁻Ag(I), respectively. The area per sulfur in this structure is 16.9 $Å^2$. This area is too small to accommodate an alkane chain with a cross sectional area of 18.4 $Å^2$. (d) The $\sqrt{39}$ R16.1°x$\sqrt{39}$ R16.1° lattice of a monolayer of silver sulfide that is also formed by the reaction of hydrogen sulfide with silver (111) (*32*). The area per sulfur in this structure is 20.4 $Å^2$.

present at the monolayer/vapor interface. SAMs can be prepared containing two components to provide greater control over the interfacial properties of the SAM (*12,24–27*). For example, SAMs derived from mixtures of thiols terminated in methyl and hydroxyl groups yield intermediate wetting properties that can be tuned to specific values by controlling the composition on the surface (see below) (*25,26*).

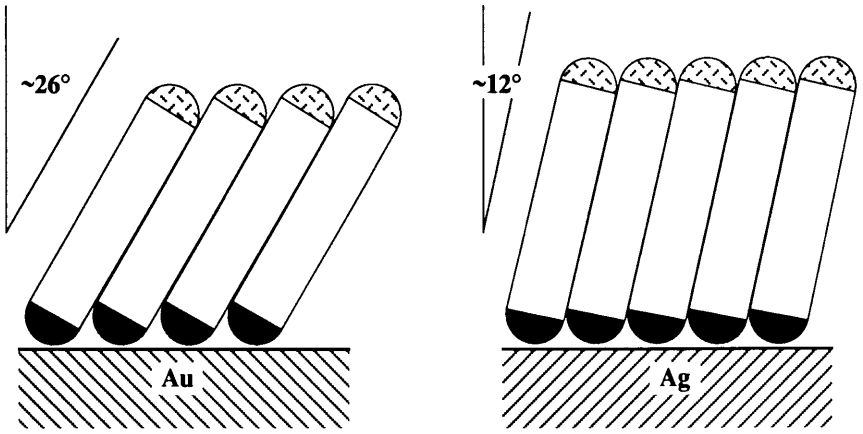

Figure 2. Illustration of the different cant angles for SAMs of alkanethiolates on gold and silver.

In addition to their utility in studies of wetting, SAMs comprising n-alkanethiolates on gold are useful model systems for studying protein adsorption to surfaces (*27*), X-ray-induced damage to organic materials (*28*), and electron transfer from fixed distances (*11,20,29*). In collaboration with Mark Wrighton's group (MIT), we have also developed a molecule-based pH sensor by incorporating an electroactive, pH sensitive group (*para*-quinone) and an electroactive reference compound (ferrocene) into the SAM (*30*).

SAMs on Silver. Silver surfaces are also highly reactive towards the adsorption of thiols (*13–15*). Silver and gold form face-centered cubic lattices with nearly identical interatomic spacings (2.88 Å and 2.89 Å for Au and Ag, respectively). Crystallites on evaporated silver surfaces also orient to present predominantly the (111) face (*15*). One would therefore predict that the structure of the SAMs formed on the two metals would be virtually indistinguishable.

Spectroscopic characterization of SAMs derived from alkanethiols adsorbed on silver using PIERS (*13,15*) and surface-enhanced Raman spectroscopy (SERS) (*14,22*) has been carried out in several laboratories; these results are in excellent agreement. In this section we focus on the results that we have obtained in collaboration with Ralph Nuzzo (AT&T Bell Labs) and David Allara (Penn State) using PIERS (*15*). Porter and co-workers have also done an excellent study on this system using PIERS (*13*).

We found the structure of SAMs derived from the adsorption of alkanethiols on silver to be related to, but different from the structure of these SAMs on gold (*15*). On both metals, the species on the surface is a thiolate, the SAM is oriented, and the alkyl chains are present primarily in a trans zig-zag conformation. On silver, however, the polymethylene chains are oriented closer to the surface normal (12° on silver vs. 26° on gold; Figure 2) and contain a lower population of gauche bonds. These observations suggest that the thiolates are more densely packed on silver than on gold (*i.e.*, the spacing between neighboring sulfur atoms is smaller on silver than it is on gold).

It is clear from the PIERS results that the sulfur atoms do not adopt the same commensurate $(\sqrt{3}x\sqrt{3})R30°$ structure that is formed on gold (111). A recent study using both grazing in-plane X-ray diffraction and low-energy helium diffraction has

shown that the structure of octadecanethiol adsorbed on silver (111) is more tightly packed than that on gold (~19.5 Å^2 vs. 21.5 Å^2) (*31*). On silver (111), the thiolates are arranged in a hexagonal array with nearest neighbor distances of ~4.7 Å, but the lattice is incommensurate with the underlying silver lattice (Figure 1b) (*31*).

We had hypothesized that the structure of thiolates on silver might be the same as one of the structures observed for an overlayer of silver sulfide formed by the reaction of H_2S with silver (111) (*15*). Of the possible structures, $(\sqrt{7}x\sqrt{7})R10.9°$ (Figure 1c) and $\sqrt{39}\,R16.1°x\sqrt{39}\,R16.1°$ (Figure 1d) seemed most probable (*32*). The former structure is observed for methyl thiolate on silver, but the packing density of this lattice is too high to accommodate a trans-extended alkyl chain (*33*). The latter structure has a lower packing density, and could accommodate a trans-extended alkyl chain with a low cant angle, relative to the surface normal (*15,32*).

Hypothesizing that the structure of alkanethiolates on silver is similar to a surface layer of silver sulfide was, however, not unreasonable. The oxide that forms on the surface of silver upon exposure to air disappears upon formation of a SAM (*15*). This observation suggests that thiolates have replaced the oxide. Clean silver surfaces will also desulfurize aromatic thiols, sulfides, and disulfides (*34*); these reactions result in the formation of a layer of silver sulfide. We have also observed that our surfaces incorporate S^{2-} species after prolonged exposure to thiol (*15*); the properties of the monolayers, however, exhibit little change. Thus, in these instances, the SAM may actually rest on a substrate of Ag_2S. Figure 1 shows that several structures are formed when hydrogen sulfide reacts with silver (111) to form a monolayer of silver sulfide; it is therefore possible that the structure formed by the adsorption of alkanethiols onto silver may depend on the experimental conditions, especially the length of time for adsorption.

SAMs of alkanethiolates on silver can also accommodate the introduction of many different tail groups (*25*). As with gold, the contact angles of water on these SAMs span a large range of wettabilities. Although the structures of SAMs on silver and gold differ in density, cant angle, and relation to the underlying substrate, the wetting properties of SAMs with common terminal functional groups on these two metals are almost indistinguishable (Figure 3). Wetting is, therefore, insensitive to the structural differences that exist between SAMs formed on gold and those formed on silver.

The formation of alkanethiolate SAMs on silver is sensitive to the degree of oxidation of the silver prior to exposure to the adsorbate. Stearic acid forms monolayers on silver oxide surfaces (*35*). While molecules of the formula $HS(CH_2)_nCO_2H$ adsorb to silver preferentially via the sulfur end as long as the surface has not oxidized significantly (*25*), both termini adsorb on silver that has been exposed to air for relatively brief periods (>5 min). These latter SAMs exhibit higher contact angles of water than those formed on silver with no oxide. To overcome these problems, exposure of the unfunctionalized silver substrates to air should be minimized; once the SAM is formed, the substrate is much less susceptible to oxidation (*15*).

SAMs on Copper. Like its congeners, copper also adsorbs alkanethiols that form oriented SAMs attached to the surface as thiolates (*15*). These samples are especially difficult to obtain in high quality, and the samples that we have examined always contained copper(I) oxide. We find this system to be extremely sensitive to the details of preparation, particularly the extent of exposure of the metal film to dioxygen (formation of a thick copper oxide) or to solution (formation of copper sulfide). Optimization of the procedure produced high-quality samples with PIERS spectra indistinguishable from those obtained on SAMs on silver (*15*). The structure of the SAMs on copper is, therefore, probably the same as that on silver: The axis of the trans-extended hydrocarbon chain is oriented close to the surface normal. Since the SAMs we characterized formed on an oxidized surface, we are hesitant to make claims

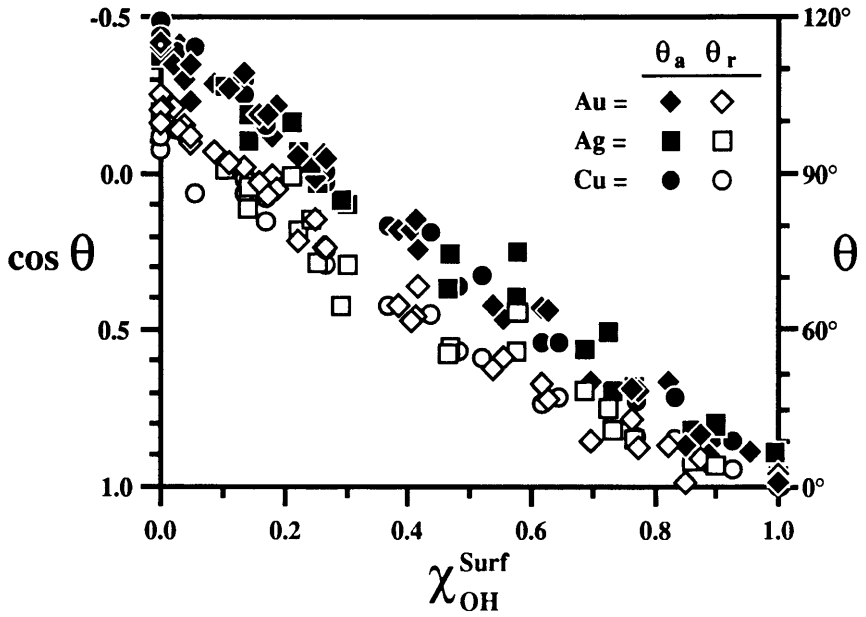

Figure 3. Advancing (filled points) and receding (open points) contact angles of water on mixed monolayers of $HS(CH_2)_{11}CH_3$ and $HS(CH_2)_{11}OH$ on gold (diamonds), silver (squares), and copper (circles). The x-axis is the mole fraction of hydroxyl-containing thiolates in the SAM as determined by X-ray photoelectron spectroscopy. The data are plotted as the cosine of the contact angles since these values are related to the interfacial free energy.

about the positions of the thiolates relative to the copper lattice. Unlike silver and gold, diffraction studies have not yet been carried out on these SAMs. On the basis of other evidence not presented here (*15*), we hypothesize that the arrangement of sulfur atoms on copper is related to copper sulfide.

Even though these SAMs form on copper oxide, they can still accommodate a wide range of polar and non-polar tail groups forming both hydrophobic and hydrophilic SAMs (*25*). As with gold and silver, SAMs derived from mixtures of thiols on copper have wetting properties that can be "tuned" to any value between those of the pure SAMs (Figure 3). The only difference between the wetting properties of mixed SAMs on the three coinage metals is that the hysteresis (the difference between the advancing and receding contact angles) increases as the substrate is changed from gold to silver to copper. This increase is probably due to an increase in the roughness of the substrate caused by oxidation of the substrate before formation of the SAM (*25*).

Summary. Self-assembled monolayers of alkanethiolates on surfaces of gold, silver, and copper have helped to illustrate differences in the chemistry of these surfaces and have clarified the relationship between the structure of a monolayer and its wetting properties (*15,25*). We are presently examining other ligands and substrates to identify surface coordination chemistries that will lead to new self-assembling systems (*36*). One of the goals of this project is to apply *the differences* between the coordination

chemistries of different surfaces to the formation of "orthogonal" monolayers (*37*) — systems that will simultaneously form different SAMs on different metal surfaces from a solution containing a mixture of ligands. These differences in adsorption can then be used to form patterned, two-dimensional organic ensembles.

Hydrogen-Bonded Networks

Background. In a self-assembled monolayer, the surface imposes a direction and orientation to the molecular ensemble, and generates a general structural motif. The three-dimensional ordering required for bulk crystallization of organic molecules is, however, usually too complicated to predict or control. A primary reason for this complexity is the great number of orientations available, in principle, to most small molecules. A number of researchers have searched for simple patterns relating molecular composition and solid structure. Leiserowitz, Etter, and McBride have respectively produced important studies on systematic functional group crystallization patterns (*38*), hydrogen-bond preferences that can be used predictively (*39*), and relationships between substituents, packing, and solid-state reactivity (*40*). Desiraju has comprehensively reviewed work on crystal engineering (*41*).

Our approach to studying the packing forces that determine three-dimensional order in crystals has been to compare the solid-state structures of a series of molecules constrained by the presence of certain functional groups. The functional groups we use are hydrogen-bond donors and acceptors, because hydrogen bonds are significantly stronger than most other interactions between small, neutral organic molecules (*42*). By restricting the number of orientational degrees of freedom of the individual molecular components with hydrogen bonds, we hoped to form crystals in which the molecules packed in regular, easily visualized arrays, and in which the substructures were relatively invariant to changes in substituents.

Stimulated by an interest in the sheet network structure proposed for the 1:1 complex between melamine and isocyanuric acid (Figure 4) (*43*), we chose to study cocrystals of derivatives of melamine (M) and barbituric acid (B). These components often form 1:1 cocrystals (eq 1). These crystals are interesting for two reasons. First,

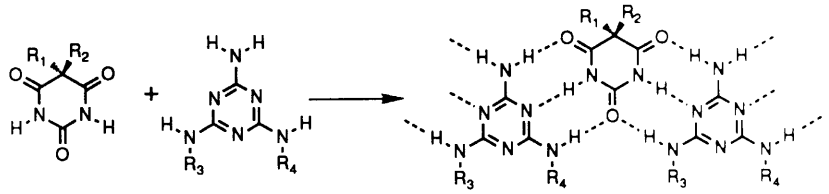

(1)

B **M**

these compounds are easily synthesized, and allow for the incorporation of a wide range of substituents into four sites (R_{1-4}) in each M·B dimer pair. Second, the hydrogen bonds between these two components significantly restrict the number of orientations the molecules can adopt in the crystals, thus limiting the number of probable substructures.

Crystalline Substructures. Figure 4 indicates that a number of structures are conceivable based on the two alternative arrangements of the three-fold hydrogen bond pattern connecting the melamine and barbiturate (isocyanurate) units. Isomerism around these sets of bonds leads to various possible substructures in the solid state, from the straight tape at the bottom of the figure to the cyclic hexamer at the top. Unless the substituents are tailored to fill interstitial voids efficiently, we suspect that

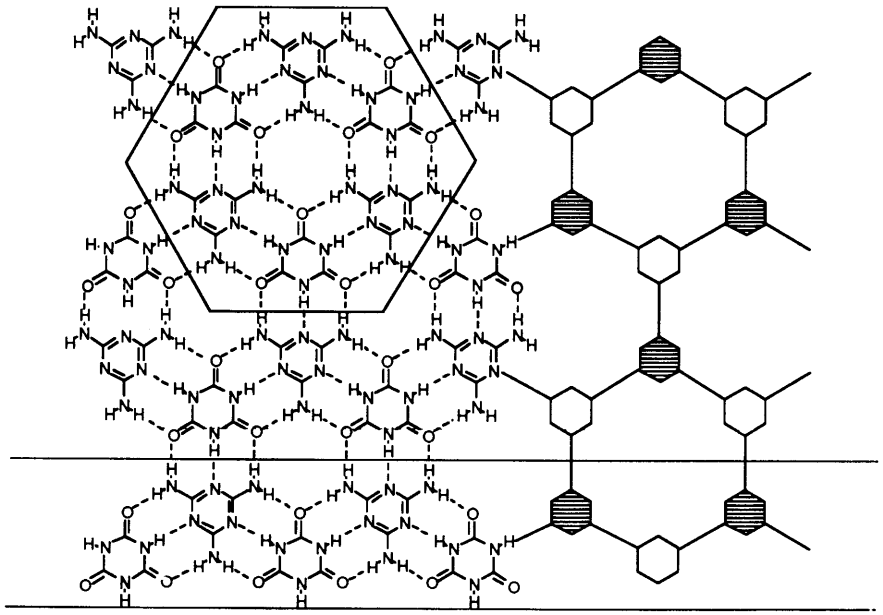

Figure 4. Portion of the proposed infinite hydrogen-bonded sheet of the complex between melamine and isocyanuric acid. Lines indicate substructures that might be obtained crystallographically by substituting parent compounds to prevent infinite hydrogen bonding.

the cyclic hexamer will rarely occur in crystals, due to the awkwardness in close packing such a shape. Several forms of tapes should, however, be accessible. We will use the nomenclature T = 1 to indicate the straight chain, where one M·B dimer unit is propagated infinitely by translation within a tape, T = 2 for a "crinkled" tape (see examples) with two dimers expressing the simplest tape unit, and so forth (Figure 5).

Once the molecules are organized at the level of tapes, they will probably undergo further assembly to some intermediate substructure. Stacking the tapes together in a venetian blind-like arrangement should give favorable close packing. Within such a stack, or sheet, the tapes could adopt a head-to-head or head-to-tail orientation. The latter would give a tape dimer that cancels dipoles; the dipoles in the former kind of stack could also cancel if the stack were adjacent to another stack in a head-to-head fashion, such as by using mirror or inversion symmetry. Analogously to our T designations, we call the head-to-head sheet S = 1, since only one orientation is translationally propagated within a stack, and the sheet consisting of head-to-tail dimers S = 2. Again, further complications are possible.

The final step for crystal construction is stacking together sheets of tapes. (We should note here that we do not expect tapes or sheets to exist as independent entities in solution; they are merely intellectual constructs intended to help visualize crystalline packing.) At this stage, sheets could line up with all their individual tapes parallel, or twisting could occur between sheets. In the absence of a strong force, such as extra hydrogen bonds that anchor a twisted configuration, we suspect that a parallel arrangement caused by the lining up of infinite ridges and valleys of substituents will be most favorable.

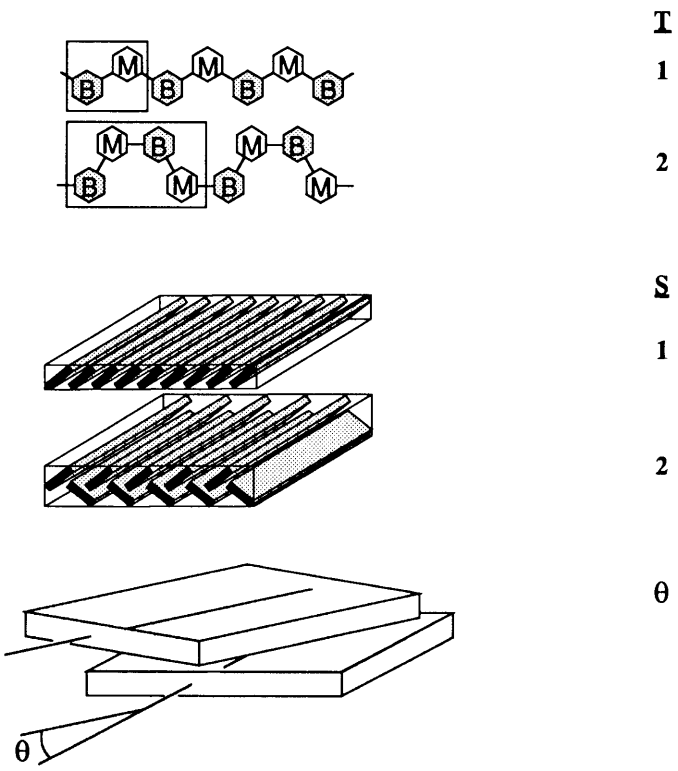

Figure 5. Crystalline substructures obtainable in 1:1 co-crystals of derivatives of barbituric acid (B) and melamine (M). T = the number of B·M dimers that constitute a translational repeat unit along a tape (boxed); S = the number of tapes that constitute a translational repeat unit in a sheet; θ = the angle between tape axes in adjacent sheets. The structures in this figure are representative examples of possible geometries and not an exhaustive list of all possible orientations of M and B.

Our approach can thus be summarized as follows: We design molecules which have firm constraints on their packing freedom, imposed upon them by intermolecular hydrogen bonds. These molecules then should repeatedly provide us with recognizable substructures of tapes and sheets in their crystals. While we expect these patterns to be formed consistently, the range of substituents available is great, so there may be significant variation between examples. We can make small perturbations on the substituent patterns and observe how, due to steric or electronic factors, the tape-tape or sheet-sheet interactions change.

Representative Examples. We have examined a large number of combinations of M and B (*42*). Most seem to form 1:1 micro-cocrystals, many of which are not large enough for single-crystal diffractometry. Nonetheless, we have been able to obtain

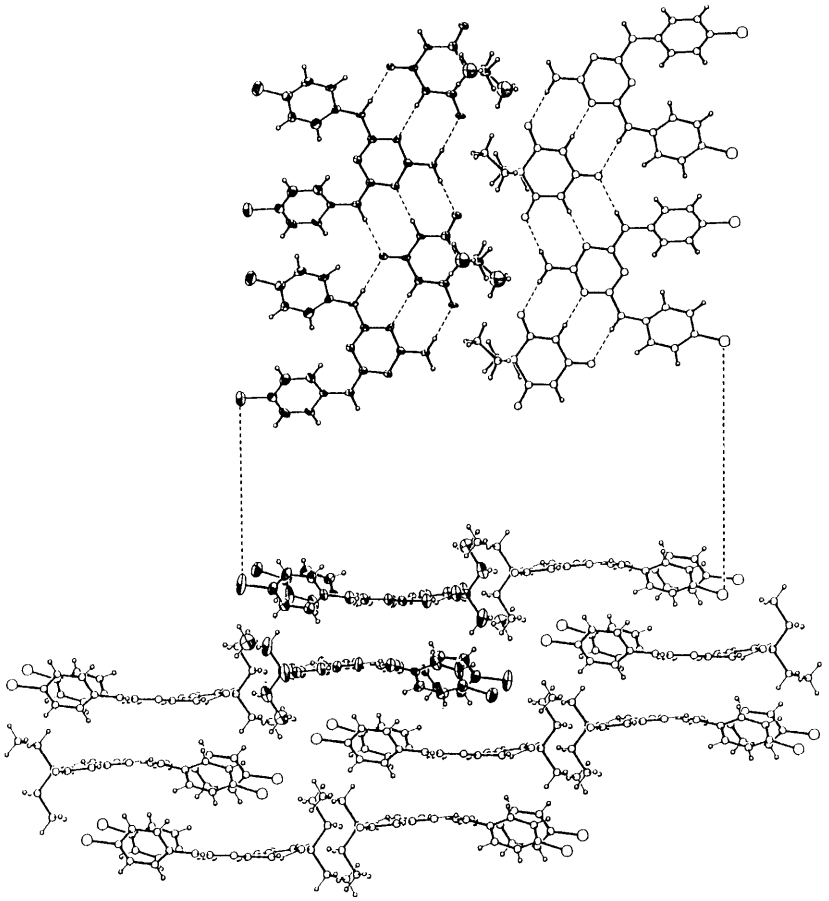

Figure 6. Bottom: End-on view of sheet packing in complex of N,N'-bis(4-chlorophenyl)melamine and barbital. A head-to-tail dimer of tapes is highlighted using thermal ellipsoids. Top: View of two tapes from the top.

structures for 21 crystals; all exist as some variant of the tape motifs summarized in Figure 5. Here we summarize only three examples to demonstrate how small changes in molecular structure can lead to large changes in tape or sheet packing. We emphasize that we have not systematically searched for polymorphisms in all of these crystallizations. We do not therefore know if the differences reflected in these three structures represent large differences in crystal energies, or smaller kinetic differences influenced by the conditions of crystallization.

The complex between N,N'-bis(4-chlorophenyl)melamine ($R_3 = R_4 =$ *p*-C_6H_4Cl) and diethylbarbituric acid (barbital; $R_1 = R_2 = CH_2CH_3$) packs as shown in Figure 6. At the top, the straight-chain nature of the tapes (T = 1) can be seen, and the bottom end-on view shows tilted sheets. Each stack consists of head-to-tail dimers of tapes (S = 2), with one of these dimers drawn using thermal ellipsoids.

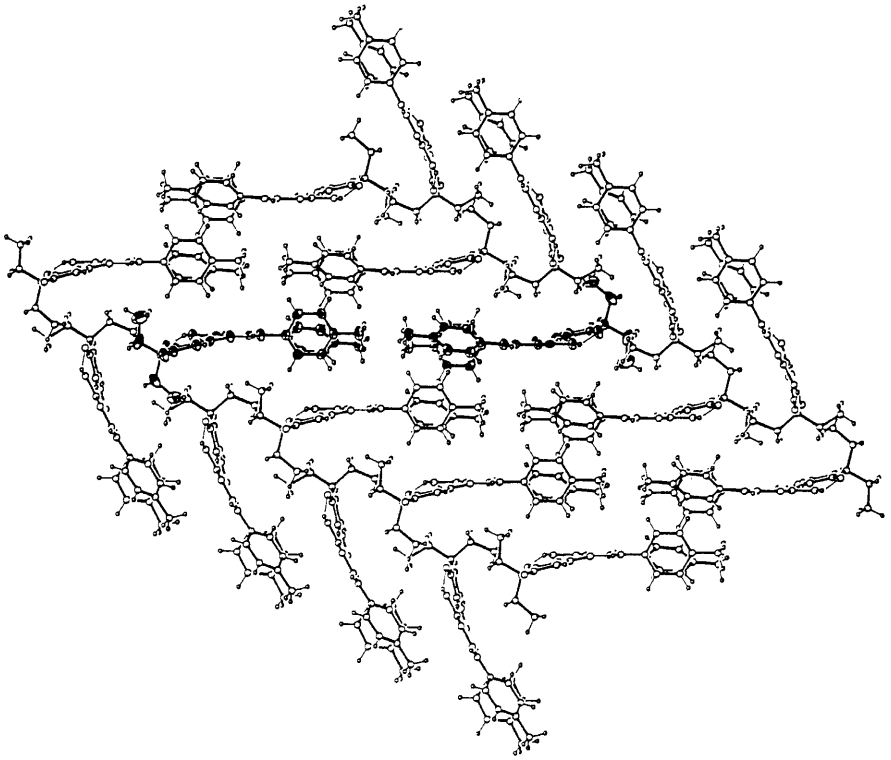

Figure 7. End-on view of sheet packing in complex of N,N'-bis(4-methylphenyl)melamine and barbital showing S = 1 packing. A head-to-head dimer of tapes is highlighted.

Changing the para-substituent from Cl to CH_3 (Figure 7) does not change the T = 1 tape format (not illustrated), but does produce a large change in the sheet architecture. Now the cancellation of dipoles is of a different type — head-to-head (S = 1) — and is inter-stack, rather than operating within one stack. One head-to-head dimer is shown in Figure 7 with thermal ellipsoids. Even though the Cl to CH_3 mutation should involve only a minimal change in volume, the steric demands might force apart head-to-tail dimers and necessitate this S = 1 packing.

Finally, moving the Cl substituent to the meta-position (Figure 8) causes a kink to appear in the chain. This crinkled form is stabilized by an intra-chain CH----O interaction, and the spacing of the tapes is apparently such as to allow incorporation of a molecule of solvent, here a well-ordered THF. The sheet architecture, while more difficult to see due to the thickness and waviness of the tapes, is still observed to be of the S = 2 dipole-cancelling type. Here, however, the "head-to-tail" dipoles are better termed "end-to-end". Within one crinkled tape (Figure 8, highlighted), the meta-chloro vectors all point in the same direction, to one end of the tape, for example toward the right of the page. In any one sheet, neighboring tapes above and below (shown in light bonds) the reference tape have their vectors pointing the other way, toward the left of the page.

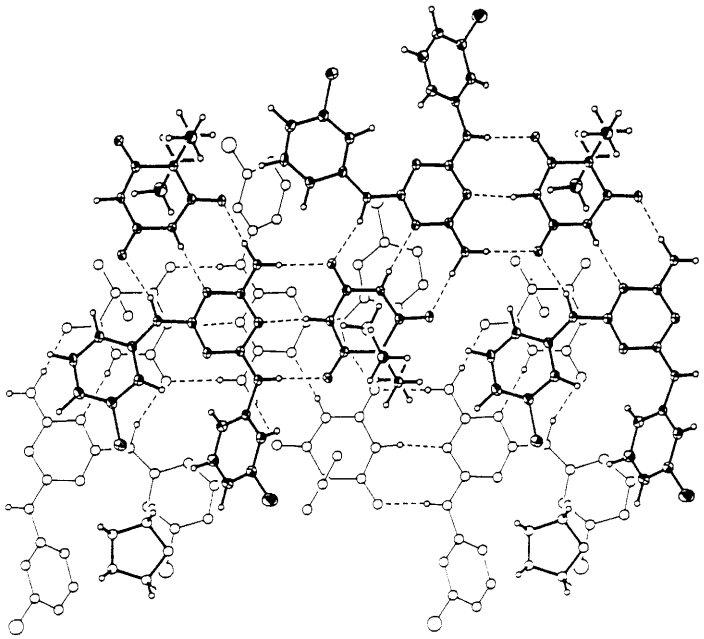

Figure 8. Two tapes of the N,N'-bis(3-chlorophenyl)melamine/barbital complex viewed from the top. The nearer tape is highlighted, and the lower one is drawn in light bonds with alkyl and aryl protons removed for clarity. Two crystallographically equivalent THF solvate molecules are shown; others have been removed.

Summary. From the results presented above (and others not discussed here), we can conclude that our basic hypothesis has been proved. The strategy for controlling the structures of crystals, provided by the network of hydrogen bonds present in the melamine/isocyanuric acid complex, but employing substituted derivatives of the parent heterocycles, has yielded crystalline substructures that can be obtained repeatedly. The motif "Tapes → Sheets → Solids" is general, and accommodates a number of pendant groups. By varying these groups, we can perturb (but not yet predict or control) the crystalline packing. Since the nature of most of the tape remains unaltered, we intend ultimately to correlate differences in packing with differences between these substituents. As we observe relationships between molecular and crystal structures over several self-consistent series (e.g. halides, alkyl chains), and with the aid of force field calculations, we hope to be able to predict crystal structures.

Acknowledgements. This research was supported by the Office of Naval Research, the Defense Advanced Research Projects Agency, and by the National Science Foundation (Grant CHE-88-12709 to G.M.W., Grant CHE 80-00670 to Harvard University for the purchase of a Siemens X-ray diffractometer, and Grant DMR-89-20490 to the Harvard University Materials Research Laboratory). J.P.F. acknowledges the National Institutes of Health for a training grant in biophysics (1989-1990). We are grateful to our many collaborators: Ralph G. Nuzzo (AT&T Bell Laboratories), David L. Allara (Penn State), Mark S. Wrighton and James J. Hickman (MIT), and Derk A. Wierda (Harvard).

Literature Cited

1. For leading references, see: Lehn, J. -M. *Angew. Chem. Int. Ed. Engl.* **1988**, *27*, 89-112. Ringsdorf, H.; Schlarb, B.; Venzmer, J. *Angew. Chem. Int. Ed. Engl.* **1988**, *27*, 113-158. Cram, D. J. *Angew. Chem. Int. Ed. Engl.* **1988**, *27*, 1009-1020. Rebek, J., Jr. *Angew. Chem. Int. Ed. Engl.* **1990**, *29*, 245-255. Sauvage, J. -P. *Acc. Chem. Res.* **1990**, *23*, 319-327.
2. Swalen, J. D.; Allara, D. L.; Andrade, J. D.; Chandross, E. A.; Garoff, S.; Israelachvili, J.; McCarthy, T. J.; Murray, R.; Pease, R. F.; Rabolt, J. F.; Wynne, K. J.; Yu, H. *Langmuir* **1987**, *3*, 932-950.
3. For some recent reviews, see: Bain, C. D.; Whitesides, G. M. *Angew. Chem. Int. Ed. Engl.* **1989**, *101*, 522-528. Whitesides, G. M.; Laibinis, P. E. *Langmuir* **1990**, *6*, 87-96.
4. Bigelow, W. C.; Pickett, D. L.; Zisman, W. A. *J. Colloid Sci.* **1946**, *1*, 513-538. Allara, D. L.; Nuzzo, R. G. *Langmuir* **1985**, *1*, 45-52, 52-66 and references therein.
5. Bartell, L. S.; Ruch, R. J. *J. Phys. Chem.* **1956**, *60*, 1231-1234. Bartell, L. S.; Ruch, R. J. *J. Phys. Chem.* **1959**, *63*, 1045-1049. Bartell, L. S.; Betts, J. F. *J. Phys. Chem.* **1960**, *64*, 1075-1076.
6. Hickman, J. J.; Zou, C.; Ofer, D.; Harvey, P. D.; Wrighton, M. S.; Laibinis, P. E.; Bain, C. D.; Whitesides, G. M. *J. Am. Chem. Soc.* **1989**, *111*, 7271-7272.
7. Troughton, E. B.; Bain, C. D.; Whitesides, G. M.; Nuzzo, R. G.; Allara, D. L.; Porter, M. D. *Langmuir* **1988**, *4*, 365-385.
8. Nuzzo, R. G.; Allara, D. L. *J. Am. Chem. Soc.* **1983**, *105*, 4481-4483. Li, T. T. -T.; Weaver, M. J. *J. Am. Chem. Soc.* **1984**, *106*, 6107-6108. Nuzzo, R. G.; Zegarski, B. R.; Dubois, L. H. *J. Am. Chem. Soc.* **1987**, *109*, 733-740.
9. Nuzzo, R. G.; Fusco, F. A.; Allara, D. L. *J. Am. Chem. Soc.* **1987**, *109*, 2358-2368.
10. Bain, C. D.; Biebuyck, H. A.; Whitesides, G. M. *Langmuir* **1989**, *5*, 723-727.
11. Porter, M. D.; Bright, T. B.; Allara, D. L.; Chidsey, C. E. D. *J. Am. Chem. Soc* **1987**, *109*, 3559-3568.
12. Bain, C. D.; Troughton, E. B.; Tao, Y. -T.; Evall, J.; Whitesides, G. M. *J. Am. Chem. Soc.* **1989**, *111*, 321-335.
13. Walczak, M. M.; Chung, C.; Stole, S. M.; Widrig, C. A.; Porter, M. D *J. Am. Chem. Soc.* **1991**, *113*, 2370-2378.
14. Bryant, M. A.; Pemberton, J. E. *J. Am. Chem. Soc.* **1991**, *113*, 3629-3637.
15. Laibinis, P. E.; Whitesides, G. M.; Allara, D. L.; Tao, Y. -T.; Parikh, A. N.; Nuzzo, R. G. *J. Am. Chem. Soc.* **1991**, *113*, 7152-7167.
16. For general examples, see: Cotton, F. A.; Wilkinson, G. *Advanced Inorganic Chemistry*; 5th Ed.; Wiley-Interscience: New York, New York, 1988. For Au(I)-sulfur interactions in solution, see: Schmidbaur, H. *Angew. Chem. Int. Ed. Engl.* **1976**, *12*, 728-740 and references therein. For a recent structural determination of RS⁻Ag(I), see: Dance, I. G.; Fisher, K. J.; Banda, H.; Scudder, M. L. *Inorg. Chem.* **1991**, *30*, 183-187.
17. Strong, L.; Whitesides, G. M. *Langmuir* **1988**, *4*, 546-558.
18. Chidsey, C. E. D.; Liu, G. -Y.; Rowntree, P.; Scoles, G. *J. Chem. Phys.* **1989**, *91*, 4421-4423.
19. Nuzzo, R. G.; Dubois, L. H.; Allara, D. L. *J. Am. Chem. Soc.* **1990**, *112*, 558-569.
20. Chidsey, C. E. D.; Loiacono, D. N. *Langmuir* **1990**, *6*, 682-691.
21. Widrig, C. A.; Alves, C. A.; Porter, M. D. *J. Am. Chem. Soc.* **1991**, *113*, 2805-2810.

22. Bryant, M. A.; Pemberton, J. E. *J. Am. Chem. Soc.* **1991**, *113*, 8284-8293.
23. Hautman, J.; Klein, M. L. *J. Chem. Phys.* **1989**, *91*, 4994-5001.
24. Bain, C. D.; Whitesides, G. M. *Langmuir* **1989**, *5*, 1370-1378.
25. Laibinis, P. E.; Whitesides, G. M. *J. Am. Chem. Soc.* submitted.
26. Bain, C. D.; Evall, J.; Whitesides, G. M. *J. Am. Chem. Soc.* **1989**, *111*, 7155-7164. Bain, C. D.; Whitesides, G. M. *J. Am. Chem. Soc.* **1989**, *111*, 7164-7175.
27. Pale-Grosdemange, C.; Simon, E. S.; Prime, K. L.; Whitesides, G. M. *J. Am. Chem. Soc.* **1991**, *113*, 12-20. Prime, K. L.; Whitesides, G. M. *Science (Washington, D.C.)* **1991**, *252*, 1164-1167.
28. Bain, C. D. Ph.D. Thesis, Harvard University, Sept. 1988. Laibinis, P. E.; Graham, R. L.; Biebuyck, H. A.; Whitesides, G. M. *Science (Washington, D.C.)* accepted.
29. Chidsey, C. E. D. *Science (Washington, D.C.)* **1991**, *251*, 919-922. Miller, C.; Cuendet, P.; Grätzel, M. *J. Phys. Chem.* **1991**, *95*, 877-886. Miller, C.; Grätzel, M. *J. Phys. Chem.* **1991**, *95*, 5225-5233.
30. Hickman, J. J.; Ofer, D.; Laibinis, P. E.; Whitesides, G. M.; Wrighton, M. S. *Science (Washington, D.C.)* **1991**, *252*, 688-691.
31. Fenter, P.; Eisenberger, P.; Li, J.; Camillone, N., III; Bernasek, S.; Scoles, G.; Ramanarayanan, T. A.; Liang, K. S. *Langmuir* **1991**, *7*, 2013-2016.
32. Schwaha, K.; Spencer, N. D.; Lambert, R. M. *Surf. Sci.* **1979**, *81*, 273-284. Rovida, G.; Pratesi, F. *Surf. Sci.* **1981**, *104*, 609-624.
33. Harris, A. L.; Rothberg, L.; Dubois, L. H.; Levinos, N. J.; Dhar, L. *Phys. Rev. Lett.* **1990**, *64*, 2086-2089. Harris, A. L.; Rothberg, L.; Dhar, L.; Levinos, N. J.; Dubois, L. H. *J. Chem. Phys.* **1991**, *94*, 2438-2448.
34. Sandroff, C. J.; Herschbach, D. R. *J. Phys. Chem.* **1982**, *86*, 3277-3279.
35. Harris, A. L.; Chidsey, C. E. D.; Levinos, N. J.; Loiacono, D. N. *Chem. Phys. Lett.* **1987**, *141*, 350-356.
36. Folkers, J. P.; Laibinis, P. E.; Whitesides, G. M. unpublished results.
37. Laibinis, P. E.; Hickman, J. J.; Wrighton, M. S; Whitesides, G. M.; *Science (Washington, D.C.)* **1989**, *245*, 845-847. Hickman, J. J.; Laibinis, P. E.; Auerbach, D. I.; Zou, C.; Gardner, T. J.; Whitesides, G. M.; Wrighton, M.S. *Langmuir* submitted.
38. Leiserowitz, L.; Hagler, A. T. *Proc. R. Soc. London* **1983**, *A388*, 133-175. Leiserowitz, L. *Acta Crystallogr.* **1976**, *B32*, 775-802.
39. Etter, M. C. *Acc. Chem. Res.* **1990**, *23*, 120-126.
40. McBride, J. M.; Segmuller, B. E.; Hollingsworth, M. D.; Mills, D. E.; Weber, B. A. *Science (Washington, D.C.)* **1986**, *234*, 830-835.
41. Desiraju, G. R. *Crystal Engineering. The Design of Organic Solids;* Elsevier: Amsterdam, 1989.
42. Zerkowski, J. A.; Seto, C. T.; Wierda, D. A.; Whitesides, G.M. *J. Am. Chem. Soc.* **1990**, *112*, 9025-9026. Zerkowski, J. A.; Seto, C. T.; Whitesides, G. M. unpublished results.
43. Seto, C. T.; Whitesides, G. M. *J. Am. Chem. Soc.* **1990**, *112*, 6409-6411. Wang, Y.; Wei, B.; Wang, Q. *J. Crystallogr. Spectrosc. Res.* **1990**, *20*, 79-84.

RECEIVED January 16, 1992

Reprinted from ACS Symposium Series No. 499
Supramolecular Architecture: Synthetic Control in Thin Films and Solids
Thomas Bein, Editor